Bishop Moore College

Mavelikara

Project Report

On

INVESTIGATION ON ANTIBACTERIAL POTENTIAL OF COPPER DOPED ZINC OXIDE NANOPARTICLES

Dissertation submitted to the University of Kerala

in partial fulfilment of the requirement for the award of the Degree of

Bachelor of Science in Physics

By

P R Rajalekshmi **Reg No: 23019101013**

Under the guidance of

Dr. ARUN ARAVIND

ASSISTANT PROFESSOR, DEPARTMENT OF PHYSICS

BISHOP MOORE COLLEGE MAVELIKARA

CERTIFICATE

This is to certify that the dissertation entitled **"Investigation on Antibacterial potential of Copper doped Zinc Oxide nanoparticles"** by **P R Rajalekshmi** (Reg. No: 23019101013)for the award of the degree of Bachelor of Science in Physics is an authentic work under my supervision and guidance during the period from 2019 – 2022.

Also certified, that the dissertation represents a team work from the part of the candidates.

Dr. Arun Aravind

Assistant Professor

Department of Physics

Bishop Moore College, Mavelikara

Examiners:

1.

2.

Declaration of Originality

I, **P R Rajalekshmi (Reg. No. 23019101013)** hereby declare that this dissertation entitled **"Investigation on antibacterial potential of copper doped zinc oxide nano particles"** represents my original work carried out as a Bachelor of Science student of University of Kerala and to the best of my knowledge, it contains no material previously published or written by another person, nor any material presented for the award of other degree or diploma of University of Kerala or any other institution. Any contribution made to this research by others, with whom I have worked at University of Kerala or elsewhere, is explicitly acknowledged in the dissertation. Work of other authors cited in this dissertation have been duly acknowledge under the section "Reference". I am fully aware that in case of non-compliance detected in future, the Senate of University of Kerala may withdraw the degree awarded to me on the basis of the present dissertation.

P R Rajalekshmi

ACKNOWLEDGEMENT

Foremost, I would like to express my sincere gratitude to my guide **Dr Arun Aravind, Assistant Professor, Bishop Moore College, Mavelikara** for his continuous support, patience, motivation, enthusiasm and most knowledge. He was always affectionate, pain taking and source of inspiration to me. His guidance helped in all the time of research and writing this project. I could not imagine having a better advisor and mentor for our research. The work could not have been possible without his worthy suggestions and constant co-operation.

Besides my advisor,I am also thankful to **Dr D Sajan, Head of the department & Assistant professor, Bishop Moore College, Mavelikara** for the help and guidance he provided to me for the initiation of this project. His Dynamism, vision, sincerity and motivation have deeply inspired me. My heart is fulfilled with deep sense of thankfulness and obeisance to our teachers for their valuable suggestions. I also express my thanks to all faculty members of Bishop Moore College, Mavelikara for their constant support.

My sincere thanks and gratitude to **Nithya S George** for her kind support during the project work. I am grateful for her inspiring and valuable suggestions during the entire period of my project work, which enabled me to complete the work successfully.

I am grateful to my parents for their love, prayers, caring and sacrifices. I also thank my friends for giving me strength.

P R Rajalekshmi

Contents

Chapter-1

INTRODUCTION

1.1 Nanoscience and Nanotechnology

Nanoscience is the study and application of structures and materials that have dimensions at the nano scale level. Nanoscience is the study of nanomaterials and their properties, and the understanding of how these materials, at the molecular level, provide novel properties and physical, chemical and biological phenomena that have been successfully used in innovative ways in a wide range of industries. Some of the unique aspects of nano systems arise solely from the tiny size of the systems. There is more to nanoscience than technology. Nanoscience is where atomic physics converges with the physics and chemistry of complex systems. Feynman's 1959 talk is often cited as a source of inspiration for Nanoscience but it was only published as a scientific paper in 1992. The remarkable technological implications laid out in Feynman's talk actually form the basis of the impression of Nanoscience for most of the people [1].

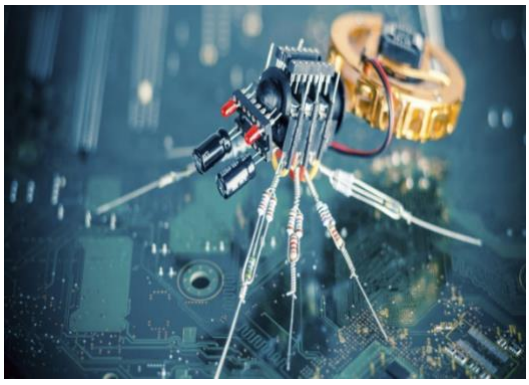

Figure 1.1 Nanochips

Figure 1.2 Viable use of nanotechnology

Nanotechnology

Nanotechnology is the science and technology of objects at the nanoscale level, the properties of which differ significantly from that of their constituent material at the macroscopic or even microscopic scale. It is a multidisciplinary field that encompasses understanding and control of matter at about 1-100 nm, leading to development of innovative and revolutionary applications. The International Standards Organization has also recently defined nanotechnology as "understanding and control of matter and processes at the nanoscale, typically, but not exclusively, below 100 nm in one or more dimensions where the onset of size-dependent phenomena usually enables novel applications, where one nanometer is one thousand millionth of a meter." Understanding the underlying science of nanoscale interactions is important to the development of technology. These interactions constitute one of the main areas of research in the field of nanotechnology.

1.2 Nanoparticles and their classification

Nanoparticles are the easiest form of structures which have the sizes in the range of Nano meter. A nanoparticle is a microscopic particle with at least one dimension less than 100 nm. Nanoparticles are of great scientific interest as they are effectively a bridge between bulk materials and atomic or molecular structures. The properties of materials change as their size approaches the Nanoscale and as the percentage of atoms at the surface of the material becomes significant. Nanoparticle have a very high surface area to volume ratio. The surface area to volume ratio also reduces the melting temperature of nanoparticles. Nanoparticle exhibit a number of special properties relative to bulk materials. For example, Copper nanoparticles smaller than 50nm are considered super hard materials that do not exhibit the same malleability and ductility as bulk copper [3].

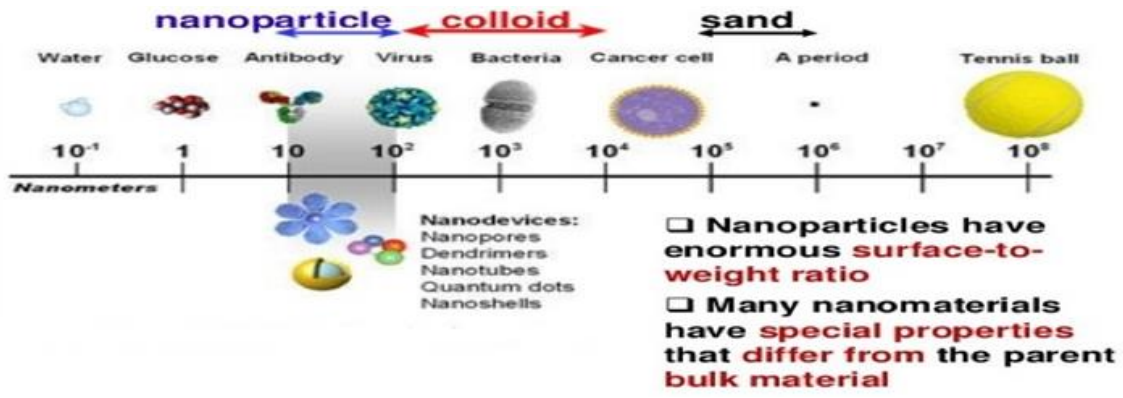

Figure 1.3 Size comparison of nanoparticles.

Control over nanoparticle size distribution and nanoparticle shape, surface properties and dispersion, aggregation stability as well as over elemental and crystalline composition is often crucial for designing new materials for specific applications. Nano film thickness, roughness and layer properties are critical parameters in thin film applications [4].

Nanoparticle shows optical properties with the variation of size and shape, it influence the absorption properties of the nanoparticle and hence different absorption colours are observed. The Lycurgus cup, when illuminated from outside, appears green. However, when illuminated from within, it glows red. The glass contains metal nanoparticles, gold and silver, which give it these unusual optical properties. The underlying physical phenomenon for this is called surface-Plasmon excitation structure. Metal nanoparticles have unique light scattering properties and exhibit Plasmon resonance. Semiconductor nanoparticles may exhibit confined energy states in their electronic band (Example: quantum dots).

1.2.1 Classification of Nanomaterials

Nanomaterial are often classified depending upon the number of the dimensions falls under Nano scale. The Nano scale is of the order of a few nanometres (1-100nm). Nanostructures can be described as zero-dimension (0D), two-dimension (2D), and three-dimension (3D) Nano material.

1.2.2 Zero dimensional nanomaterials

In this, all dimensions are reduced to nm range, movement of electron is restricted in all three x, y, and z directions. The most common representation of zero dimensional nanomaterial's are nanoparticles. Nanoparticles can be amorphous, single crystalline composed of single or multi chemical elements which exhibits various shapes and forms exist individually or in a matrix be metallic, ceramic or polymeric. Examples: Fullerene, Nano gold, Quantum dots etc.

1.2.3 One dimensional nanomaterials

One dimension that is outside the Nano scale. This leads to needle like shaped nanomaterial. 1D nanomaterial can be amorphous or crystalline which is made up of single or polycrystalline. They are chemically pure or impure seen in standalone material or embedded in within another medium [5]. Examples: Carbon Nanotubes, Nano fibres etc.

1.2.4 Two dimensional nanomaterials

Two of the dimensions are not confined to the Nano scale. This nanomaterial's exhibit plate-like shapes. 2D nanomaterial can be amorphous which is made up of various chemical compositions. It can be used as single layer or as multilayer structures exist in surrounding matrix material be metallic, ceramic or polymeric. Examples: Nano films, Nano coatings etc.

1.2.5 Three dimensional nanomaterials

Nanomaterial's which have all dimensions outside nanoscale range, but perform nanomaterial properties. Three dimension nanomaterial most widely used in magnetic materials, catalysts, and so on. It is evident that behaviour of 3D nanomaterial is purely based on shapes, size, morphologies and dimension. Examples: Nanocomposites, Nanostructured films etc.

1.3 Properties of Nanoparticles

The properties of a material in nanoparticle form are usually different from those of the bulk one even when divided into micrometer size particles. Many of them arise from spatial confinement of sub atomic particles like electrons,protons,photons.

Large area/volume ratio : A bulk materials are expected to have constant physical properties such as thermal and electrical conductivity,density,viscocity regardless of size for nano particle this is different , the volume of the surface layer becomes a significant fraction of the particle's volume.

Solvent affinity : Suspensions of nanoparticles are possible since the interaction of the particle surface with the solvent is strong enough to overcome density differences , which otherwise usually result in a material either sinking or floating in a liquid.

Diffusion across the surface : The high surface area of a material in nanoparticle form allows heat ,molecules and ions to diffuse into or out of the particles at very large rates .

Melting point depression : A material may have lower melting point in nanoparticle form than in the bulk form. For example,2.5 nm gold nanoparticles melt at about 300 degree celsius,whereas bulk gold melts at 1064 degree Celsius.

1.4 Synthesis approach for Nanoparticle preparation

In the synthesis of nanoparticles, which can be natural or synthetic origin and exhibit unique properties at the nanoscale, two basic approaches that include various preparation methods. The approaches are top-down and bottom-up.

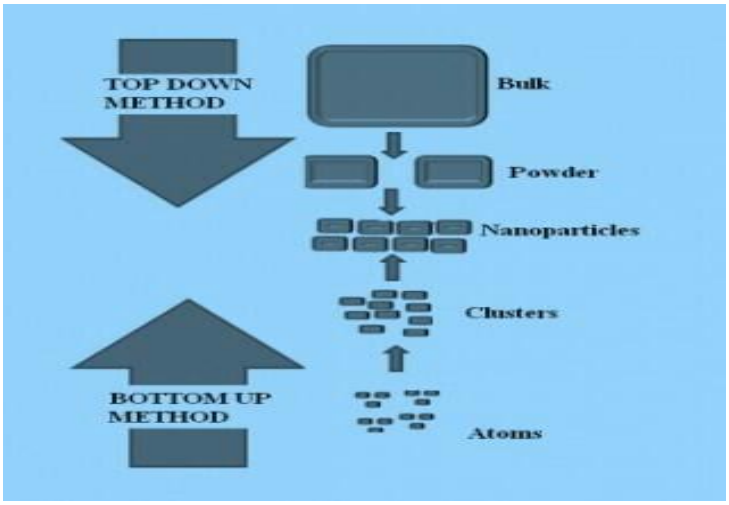

Figure1.4 : Top down and bottom up approach

1.4.1 Top Down Approach

The top-down method is based on breaking down of solid materials into small pieces by applying external force. In this approach, many physical, chemical and thermal technique are used to provide the necessary energy for nanoparticle formation. Although this method is inexpensive, efficient and simple.

1.4.2 Bottom Up Approach

The bottom up method is based on gathering and combining gas or liquid atoms or molecules. In this approach, no waste materials that need to be removed are formed, and nanoparticles having smaller size can be obtained by better control of sizes. Molecular components arrange themselves into some useful conformation using the concept of molecular self-assembly. Example: Synthesis of nanoparticles by colloid dispersions.

1.5 Introduction to Transition metal oxide

Transition metal oxide nanoparticles have received a growing attention in the field of materials science because of their size and shape dependent physicochemical and functional properties .One of the promising applications of transition metal oxides is their ability to degrade wide varieties of organic dyes in the presence of sunlight or uv light radiation.

1.5.1 ZnO Nanostructures

ZnO is a versatile functional material that has a diverse group of growth morphology, such as nanocombs, nanoring's, nanosprings, nanobelts, nanowires and nanocages. ZnO is a wide band gap (3.37 eV) compound semi conductor that is suitable for short wavelength optoelectronic applications. The high exciton binding energy(60 meV) in zinc oxide crystal can ensure efficient

excitonic emission at room temperature and ultraviolet luminescence has been reported in nanoparticles. ZnO is transparent to visible light and can be made highly conductive by doping.

1.5.2 Crystal and surface structure of ZnO

Wurtzite ZnO has a hexagonal structure with lattice parametres a =0.3296 and c =0.52065nm.The structure of ZnO can be simply described as a number of alternating planes composed of tetrahedrally coordinated oxygen and zinc ions, stacked alternately along the c- axis. Tetrahedral coordination in ZnO results in non central symmetric structure and consequently piezoelectricity and pyroelectricity. Another important characteristic of ZnO is polar surfaces .The most common polar surface is the basal plane. The oppositely charged ions produce positively charged Zn+ and negatively charged O- surfaces, resulting in a normal dipole moment and spontaneous polarization along the c-axis as well as a divergence in surface energy. To maintain a stable structure, the polar surfaces generally have facets or exhibit massive surface reconstructions, but ZnO are exceptions: they are atomically flat, stable and without reconstruction . Efforts to understand the superior stability of the ZnO polar surfaces are at the forefront of research in today's surface physics .

1.5.3 Applications of ZnO nanoparticles

ZnO nanoparticles are used in an increasing number of industrial products such as rubber, paint, coating and cosmetics. ZnO nanoparticles have several advantages : high antibacterial effectiveness at low concentrations(0.16-5.00mmol/L),activity against a wild range of strains, relatively low cost. The antimicrobial activity of ZnO is an ability of metal ions to inhibit enzymes, facilitate reactive oxygen called the fenton reaction, causes the damage of cell membranes ,prevent the uptake of vitally important microelements by microbes

Agricultural applications of zinc oxide

ZnO nanoparticles have potential to enhance the growth of food crops. Seeds fixed by various ZnO nanoparticles concentrations improved seed propagation , seed strength and plant growth. ZnO nanoparticles showed to be active in growing roots ,stems and seeds.

Medicinal applications

ZnO nanoparticles have certain properties that make them appropriate for applications associated with central nervous system. ZnO influenced unalike tissues, cell sore functions, as well as neural tissue engineering and biocompatibility.

Field effect transistor

Field effect transistors have been fabricated using individual nanobelts. Large bundles of ZnO nanobelts where dispersed in ethanol by ultrasonication until mostly individual nano belts were isolated. Here the fabrication is done by depositing dispersed ZnO nanobelts on redefined gold

electrode arrays. The electron arrays are variably spaced a typical ZnO Field effect transistor showed a gate threshold voltage of -15V and a switching ratio of nearly 100.

Chapter 2

LITERATURE REVIEW

S.Muthukumaran et al[1], reported the synthesis of Cu doped ZnO nanopowders by co-precipitation method and annealed at 500 degree Celsius for 2 hours under Ar atmosphere. The synthesized samples have been characterized by powder X-ray diffraction, energy-dispersive analysis X-ray (EDAX) spectra, UV–Visible spectrophotometer and Fourier transform infrared (FTIR) spectroscopy. The XRD measurement reveals that the prepared nanoparticles have different microstructure without changing a hexagonal wurtzite structure. The calculated average crystalline size decreases from 22.24 to 15.93 nm for x = 0 to 0.04 then reaches 26.54 nm for x = 0.06 which is confirmed by SEM micrographs. The change in lattice parameters, micro-strain, a small shift and broadening in XRD peaks and the reduction in the energy gap from 3.49 to 3.43 eV reveals the substitution of Cu2+ ions into the ZnO lattice. Hydrogenation effect improves the crystal quality and optical properties. It is proposed that Cu doping concentration limit is below 6% (0.06) molar fraction which is supported by the detailed XRD analysis and the derived structural parameters. This Cu concentration limit was proposed as below 5% by previous studies. The presence of functional groups and the chemical bonding is confirmed by FTIR spectra.

Thomas et al[2], reported the synthesis of ZnO nanoparticles by hydrothermal method. Structural properties of synthesized sample was studied by using X-ray diffraction (XRD) and exact fitting of peaks was done by using Rietveld Refinement with Crystallographic Open Database(COD).It reveals that ZnO nanostructures follows a hexagonal wurtzite structure with P-63mn space group. Williamson-Hall (W-H) plot method was used to determine the value of lattice strain and crystallite size on the samples.. Optical properties and bandgap values of ZnO was verified by using UV-Visible spectroscopy and Photoluminescence (PL) spectroscopy respectively. Morphological properties and elemental composition were studied by using Field Emission Scanning Electron Microscopy (FESEM) and Energy Dispersive Spectroscopy (EDS) respectively. The oxidation states of the elements are determined by using X-ray photoelectron Spectroscopy (XPS).Adsorption capacity and photocatalytic degradation of malachite green dye using ZnO nanostructures as photocatalyst is verified.

Jose et al[3], the growth of phase pure ZnO nanostructures from Aloe-Vera leaf extract and degradation of an organic dye-Malachite Green (MG)- from aqueous medium using the same as

catalyst. Adsorption mechanisms were evaluated using Lagergren's pseudo-first-order, pseudo-second-order and intraparticle diffusion kinetic models. X-Ray diffraction data showed that the synthesised ZnO is crystalline with hexagonal wurtzite phase. Average crystallite size and lattice strain was estimated from Scherrer equation and Williamson-Hall analysis with the help of Rietveld refinement data. Crystallite size obtained from Scherrer method is 12.62 nm while that from Williamson-Hall analysis is 19.27 nm. Uniform growth of ZnO nanosheets were confirmed by FE-SEM analysis. Optical characterisation was carried by UV-Visible spectroscopy and the band gap ZnO nanoparticles was found to be 3.19 eV. ZnO stretching vibrations were recorded at 550 cm−1 using FTIR spectrophotometer. Results showed that biosynthesised ZnO nanosheets are particularly effective for the degradation of MG dye

Mohan et al [4] synthesized ZnO nanoparticles by hydrothermal method under different conditions and studied various properties. FTIR studies proved the presence of ZnO bonding and purity of the samples. Grain size was found to be decreased with the increase of reaction temperature and increased with reaction time. TEM images show formation of nanorods under same reaction temperature, also nanoflowers and nanospheres for different temperatures. Intensity of luminescence peaks is found to be changed with variation in interplanar spacing. UV–vis spectra helped to identify the increased photon absorption in particles of bigger size. Change in bandgap value is also observed due to the difference in size of nanoparticles.

Safari et al[5]. Cu-doped ZnO nanoparticles were investigated as an efficient synthesized catalyst for photodegradation of humic substances in aqueous solution under natural sunlight irradiation. Cu-doped ZnO nanocatalyst was prepared through mild hydrothermal method and was characterized using FT-IR, powder XRD and SEM techniques. The effect of operating parameters such as doping ratio, initial pH, catalyst dosage, initial concentrations of humic substances and sunlight illuminance were studied on humic substances degradation efficiency. The results of characterization analyses of samples confirmed the proper synthesis of Cu-doped ZnO nanocatalyst. The experimental results indicated the highest degradation efficiency of HS (99.2 %) observed using 1.5 % Cu-doped ZnO nanoparticles at reaction time of 120 min. Photocatalytic degradation efficiency of HS in a neutral and acidic pH was much higher than that at alkaline pH. Photocatalytic degradation of HS was enhanced with increasing the catalyst dosage and sunlight illuminance, while increasing the initial HS concentration led to decrease in the degradation efficiency of HS. Conclusively, Cu-doped ZnO nanoparticles can be used as a promising and efficient catalyst for degradation of HS under natural sunlight irradiation.

B Saad et al[6] reported, Pure and Cu-doped zinc oxide nanoparticles were prepared via hydrothermal synthesis using a solution of zinc sulfate (ZnSO4) as precursor, p-phenylenedi-amine as structure-directing agent in the presence of different amounts of CuSO4 and NaOH. XRD, Raman, UV–Vis, and PL techniques were used to characterize the as-synthesized samples. The XRD analysis reveals that the average particle size of pure ZnO is 13.50 nm. It decreased to 12.11 nm for the Cu-doped sample ZnO then to 11.00 nm when x = 0.15. The optical band gap of pure and Cu-doped ZnO nanoparticles was calculated from UV–Vis spectra. It turned out to have decreased from 3.18 to 3.11 eV.

Chapter 3

CHARACTERIZATION TECHNIQUES

The measurement and characterization of nanoscale objects have always been a technical and metrological challenge. The developments in nanotechnology analysis and metrology over the last few years however, allowed for continuously smaller nanoscale dimensions to be measured and controlled. In order to determine the nanoparticles specific properties we apply different characterization and analytical method depending on the physical or chemical quantity to be determined.

1)X-Ray Diffraction Technique(XRD)

2) Field Emission Scanning Electron Microscopy (FESEM)

3)UV- spectroscopy

3.1 POWDER X - RAY DIFFRACTION (XRD)

X - ray diffraction technique is the most common and efficient method for the determination of structure and crystallinity and material identification. XRD is an apt method to examine whether a resultant material has amorphous or crystalline nature. Crystalline phases can be identified by just comparing the interplanar distance ‘d’ values obtained from XRD data with the fundamental data in Joint Committee on Powder Diffraction Standards (JCPDS).

3.1.1 Principle

X - ray diffraction is based on constructive interference of monochromatic X - rays from a crystalline sample. The X - rays, generated by a cathode ray tube are filtered to produce monochromatic radiation, collimated and directed towards the sample. X - ray primarily interact with electrons in atoms, collide and some photons from the incident beam are deflected away from original. The X - rays interfere constructively and destructively producing a diffraction pattern on the detector. The incident X - ray radiation produces a Bragg peak if their reflections from the various planes interfered constructively. The interference is constructive, when the phase shift is a multiple of 2π, this condition can be expressed by Bragg's law

$n\lambda = 2d \sin\theta$

where n is an integer, λ is the wavelength of incident wave, d is the spacing between the planes in the atomic lattice and θ is the angle between the incident ray and the scattering planes. Schematic diagram of X - ray diffraction is shown in Figure

3.1.2 Bragg's Law

When a crystal is bombarded with X-Rays of the fixed wavelength (similar to spacing of the atomic scale lattice planes)and at certain incident angles,intense reflected X-Rays are produced when the wavelengths of scattered X-Rays interference constructively,the differences in the travel path must be equal to integer multiples of the wavelength,When this constructive interference occurs,a diffracted beam of X-Rays will leave the crystal at an angle equal to that of the incident beam.To illustrate this feature,consider a crystal with crystal lattice planar distances d(right).Where the travel path length difference between the paths.ABC and A'B'C' is an integer multiple of wavelength,constructive interference will occur for a combination of the specific wavelength,crystal lattice planar spacing,and angle of incidence(θ).Each rational plane of atoms in a crystal will undergo refraction at single,unique angle(for X-Rays of a fixed wavelength). The general relationship between the wavelength of the incident XRays ,angle of incident and spacing between the crystal lattice planes of atoms is known as Bragg's Law is given by,$n\lambda=2d\sin\theta$ where n(an integer) is the "order" of reflection.λ is the wavelength of the incident X-Rays,d is the interplanar spacing of the crystal and θ is the angle of incidence. Bragg's Law states the X-Rays reflected from different parallel planes of a crystal constructively when the path difference is integral multiple of the wavelength of x-rays.

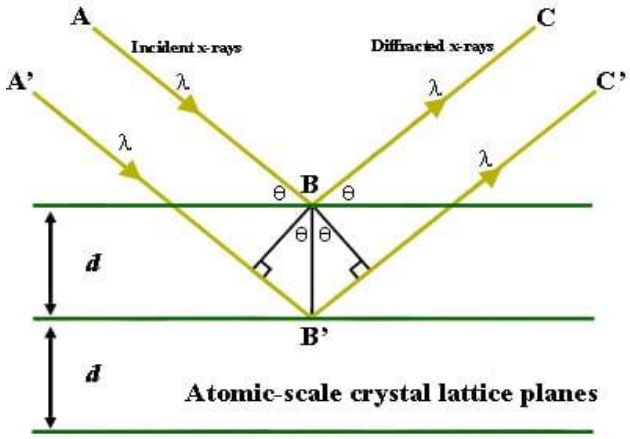

Figure 3.1 Bragg's law

3.1.3 Instrumentation

A typical powder X - ray diffractometer consists of a source of radiation, a monochromator to choose the wavelength, slits to adjust the shape of the beam, a sample and a detector. A goniometer is used for fine adjustment of the sample and the detector positions. The goniometer mechanism supports the sample and detector, allowing precise movement. The source X - rays contains several components; the most common being Kα and Kβ. The specific wavelengths are characteristic of the target material (Cu, Fe, Mo, Cr). Monochromators and filters are used to absorb the unwanted emission with wavelength Kβ, while allowing the desired wavelength, Kα to pass through. The X - ray radiation most commonly used is that emitted by copper, whose characteristic wavelength for the Kα radiation is equal to 1.5418 Å. The filtered X - rays are collimated and directed onto the sample as shown in the Figure . When the incident beam strikes a powder sample, diffraction occurs in every possible orientation of 2θ. The diffracted beam may be detected by using a moveable detector such as a Geiger counter, which is connected to a chart recorder. The counter is set to scan over a range of 2θ values at a constant angular velocity. Routinely, a 2θ range of 5 to 70 degrees is sufficient to cover the most useful part of the powder pattern. The scanning speed of the counter is usually 2θ of 2° min-1 . A detector records and processes this X - ray signal and converts the signal to a count rate which is then fed to a device such as a printer or computer monitor. The sample must be ground to fine powder before loading it in the glass sample holder. Sample should completely occupy the square glass well. In the present work, XRD patterns were recorded using X'per PRO PAN analytical and Rigaku X - ray diffractometer (RINT - 2200) with CuKα radiation at 0.02° / sec step interval.

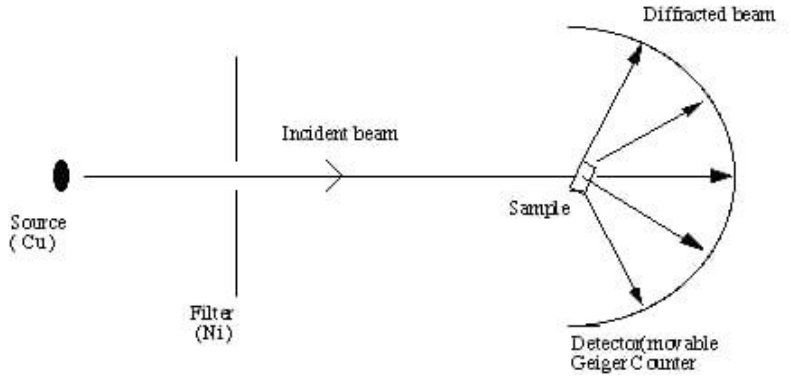

Figure 3.2 Powder Diffraction Method

X-Ray powder diffraction is most widely used for the identification of unknown crystalline materials.

Other applications are include:

 Characterizations of crystalline materials

 Determination of unit cell dimensions

 Measurements of sample purity

 With specialized technique ,XRD can be used to:

 Determination crystal structures using Rietveld refinement

 Determine of model amounts of minerals(quantitative analysis)

 Characterize thin samples by:

a)Determine lattice mismatch between film and substrate and to inferring stress and strain.

b)Determining dislocation density and quality of the film by ricking curve measurements.

c)Measuring super lattices in multilayered epitaxial structures.

d)Determining the thickness,roughness,and density of the film using glancing incidence X-ray reflectivity measurements.

e)Make textual measurements ,such as the orientations of grains ,in a polycrystalline sample.

3.2 Field Emission Scanning Electron Microscopy[FESEM]

Field emission scanning electron microscopy (FESEM) provides topographical and elemental information at magnifications of 10x to 300,000x, with virtually unlimited depth of field. Compared with convention scanning electron microscopy (SEM), field emission SEM (FESEM) produces clearer, less electrostatically distorted images with spatial resolution down to 1 1/2 nanometers – three to six times better.

Principle

A FESEM is microscope that works with electrons (particles with a negative charge) instead of light. These electrons are liberated by a field emission source. The object is scanned by electrons according to a zig-zag pattern.

Working:

Electrons are liberated from a field emission source and accelerated in a high electrical field gradient. Within the high vacuum column, these so-called primary electrons are focused and deflected by electronic lenses to produce a narrow scan beam that bombards the object. As a result, secondary electrons are emitted from each spot on the object. The angle and velocity of these

secondary electrons relate to the surface structure of the object. A detector catches the secondary electrons and produces an electronic signal. This signal is amplified and transformed to a monitor or to a digital image that can be saved and processed.

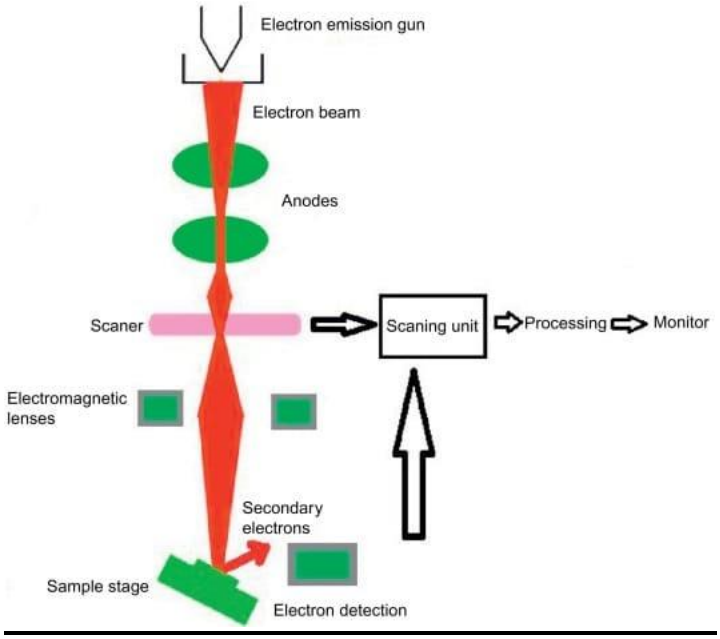

Figure 3.1 FESEM

The FESEM looks like a cylindrical column mounted on a desk. The column hosts the electron beam. Knobs for the regulation of the electron beam can be found at various levels on the column. The microscope is operated from the steering panel. A copy of this panel has been used for the simulations.

Advantages of FESEM include:

The ability to examine smaller-area contamination spots at electron accelerating voltages compatible with energy dispersive spectroscopy (EDS). Reduced penetration of low-kinetic-energy electrons probes closer to the immediate material surface. High-quality, low-voltage images with negligible electrical charging of samples (accelerating voltages ranging from 0.5 to 30 kilovolts). Essentially no need for placing conducting coatings on insulating material.

Applications: Applications of FESEM include:

Semiconductor device cross section analyses for gate widths, gate oxides, film thicknesses, and construction details advanced coating thickness and structure uniformity determination Small contamination feature geometry and elemental composition measurement.

3.3 UV - VISIBLE SPECTROSCOPY

This refers to absorption spectroscopy in the ultra - violet and visible spectral region. In this region of the electromagnetic spectrum, molecules undergo electronic transition. When sample molecules are exposed to light having an energy (E = hυ where 'E' is energy in joules, 'h' is Planck's constant 6.62×10^{-34} J s and υ is frequency in Hertz), that matches a possible electronic transition within the molecule, some of the light energy will be absorbed as the electron is promoted to a higher energy orbital. An optical spectrometer records the wavelengths at which absorption occurs, together with the degree of absorption at each wavelength. The resulting spectrum is presented as a graph of absorbance (A) versus wavelength (λ). The optical properties of materials can be studied with the help of UV - Vis spectra.

3.3.1 Principle

The absorbance of light by molecules in the solution is based on the Beer - Lambert law, A=log I0/I=ε *b*c where, I0 is the intensity of the reference beam and I is the intensity of the sample beam,ε is the molar absorbtivity with units of L mol- 1 cm - 1 , b = path length of the sample in centimeters and c = concentration given solution expressed in mol L - 1 .

3.3.2 Instrumentation

The main components of the UV - Vis spectrometers are a light source, double beams (reference and sample beam), a monochromator, a detector and a recording device. The source is usually a tungsten filament lamp for visible and deuterium discharge lamp for UV measurements. The light coming out of the source is split into two beams - the reference and the sample beam as shown in the Figure 2.3. The sample and reference cells are rectangular quartz / glass containers; they contain the solution (to be tested) and pure solvent, respectively. The spectrometer records the ratio between the reference and sample beam intensities. The recorder plots the absorbance (A) against the wavelength (λ). The sample is prepared into a paste and then dissolved into the solvent to make a dilute sample solution. This sample solution is filled up to mark line of the sample cell. In the present work, UV - visible absorption analyses were performed by Varian Cary 5E UV - Vis - NIR spectrophotometer and Shimadzu (Japan) 3100 PC spectrophotometer using ethanol as a dispersing medium.

Chapter 4

SYNTHESIS OF NANOPARTICLES

4.1 Hydrothermal method

Hydrothermal synthesis method involves using any one of the many techniques to crystallize substances. It usually does at a high vapor pressure level and using a high-temperature aqueous solution; hence it is termed as 'Hydro' + 'Thermal' = Hydrothermal method. We have observed natural process for more than 800 years now and the term has geological origins. Hydrothermal method is a standard preparation route, especially for powdery nanostructure. Hydrothermal synthesis refers to the heterogeneous reactions for synthesizing inorganic materials in aqueous media above ambient temperature and pressure. In this case, an aqueous mixture of precursors is heated in a sealed stainless-steel autoclave above the boiling point of water, and consequently the pressure within the reaction autoclave is dynamically increased above atmospheric pressure. This effect of high temperature and pressure provides a one step process to produce highly crystalline materials without the need of post annealing treatment. The hydrothermal synthesis could obtain magnetic nanomaterials with very high crystallinity due to their high temperature and high-pressure reaction conditions. Hydrothermal method have several advantages such as low cost, easy experimental setup, and high yield.

Figure 4.1 Autoclave Reactor

As a result of the main thermodynamic and kinetic features of the hydrothermal process, the main advantages of the hydrothermal synthesis are:

- One step process for powder synthesis or oriented ceramic films
- Minimized consumption of energy, particularly for complex and doped oxides
- Products with much high homogeneity than solid state processing
- Products with higher density than gas or vacuum processing
- One of the few methods enabling for obtaining of controlled doped or complex material system

Hydrothermal technique for nanoparticle synthesis needs using special instrumentation, called Hydrothermal Autoclave Reactor. It is a specific style of strong vessel that we intend to face up to high temperatures and better pressure levels from within.

The autoclave reactor consists of thick and steel-walled cylindrical vessels having hermetic sealing. Likewise, this helps it to bear high levels of heat and pressure regularly and safely, for a long time. Also, the fabric of the autoclave also must be resistant to solvents. While the most vital part of the hydrothermal autoclave reactor is probably the ‘closure’. Apart from this, the seals are a successive necessary part of the autoclave.

As many hydrothermal processes need to use solutions having a corrosive impact on the interior material of the autoclave. Also, we apply special protective coatings to prevent corrosion. Because we usually design to suit the interior of the autoclave seamlessly and can either cover the entire interior of the autoclave or part of it.

Figure 4.2 Teflon Beaker

Advantages of Hydrothermal Synthesis

Method for Nanoparticle Synthesis:These are some of the top advantages and advantages of using hydrothermal nanoparticle synthesis methodology, as compared to other ways, for crystallization and synthesis of nanomaterials: Able to produce crystalline phases which aren't stable at higher temperatures safely. Grows materials which are known to have a higher vapor pressure as their melting point gets closer. Creates larger-sized and high-quality crystals and nanoparticles, with control over their content and composition.

4.2 Materials and synthesis of Cu doped ZnO by hydrothermal method:

The semiconductor nanomaterials are of great interest. They have attracted much research in recent years because of their possible applications in field of such as gas sensors, solar cells , field-effect transistors (FETs) , electronics and opto-electronics . ZnO is also comparable with other large band gap semiconductors, such as SiC and GaN [7]. In addition, the high binding energy of the free exciton of ZnO (about 60 meV) [8, 9] and its high melting point (2250 K) make it potentially very effective in excitonic emission devices, as this gives it good high tempera- ture operating stability and makes it a better material than GaN. However, the essential lock of ZnO is to obtain stable and reproducible p-type doping. This obstacle significantly hinders the development of ZnO technology for optoelectronic components.

ZnO and 2.5% Ni doped ZnO nanorodes were grown by simple hydrothermal route. 1M zinc acetate dihyderate($(CH3.CO_2)_2$ $Zn.2H_2O$) soulution was prepared initially to which an appropriate

amount of ammonium hydroxide was added to maintain the pH at 11. Ni doped ZnO nanostructures was prepared by adding a known amount of nickel acetate tetrahyderate($(CH3.CO_2)_2$ $Ni.4H_2O$). The mixture was stirred vigorously for 30 minutes to form a homogeneous solution and was transferred into Teflon lined stainless steel autoclave and maintained at 150 degree celsius for 2 hours . After the desired reaction time,it was allowed to cool naturally to room temperature.Resulting products were washed with methanol ,filtered and then dried in air in a laboratory oven at 60 degree celsius .

Chapter 5

RESULT AND DISCUSSION

XRD analysis

Structural characterization of synthesized samples, determined from XRD diffraction pattern are shown in Fig 1. The obtained XRD patterns of Pure and Cu doped ZnO seems to be matching. The sharp diffraction peaks indicate the highly crystalline nature of the material as reported earlier. Peaks observed at 2θ values of 31.52º, 34.15º, 35.95º, 47.28º, 56.28º, 62.52º, 66.11º, 67.68º, 68.83º, 72.22º and 76.84º which corresponds to the ZnO crystal planes. Major diffraction peaks at (100), (002) and (101) planes is in well agreement with the hexagonal wurtzite ZnO crystal structure (JCPDS No. 36-1451) which is the most stable phase of ZnO, space group of P63mc [7].Since there is no other peaks seems corresponding to copper, which indicates the proper substitution of Cu over the Zinc sites since the ionic radii of Cu^{2+} (0.73Å) and Zn^{2+}(0.74Å) are comparably same. By Debye Scherrer formula from the full width half maximum of the peaks, the crystalline size of the samples can be found. Average crystalline size calculated from Debye Scherrer formula as follows[8]:

$$D = \frac{0.9\lambda}{\beta\cos\theta}$$

Where D is the average crystalline size in nm, λ is the wavelength of Xray(1.5141Å), θ is the Braggs angle in degrees and β full width half maximum(FWHM) in radians. Compared to pure ZnO, crystalline size found to decrease. The decrease in crystalline size may due to Cu^{2+} addition which decreases the nucleation and growth rate. The existence of Cu^{2+} ions in ZnO lattice restricted the crystal grain size increment. For doped samples, the increase in strain compared to the pristine ZnO causes increase in lattice constants and thereby there is a decrease in particle size observed[9] .

For convenience, the samples were named correspondingly as Zn and CZ for pure ZnO and 5% Cu doped ZnO nanoparticles respectively.

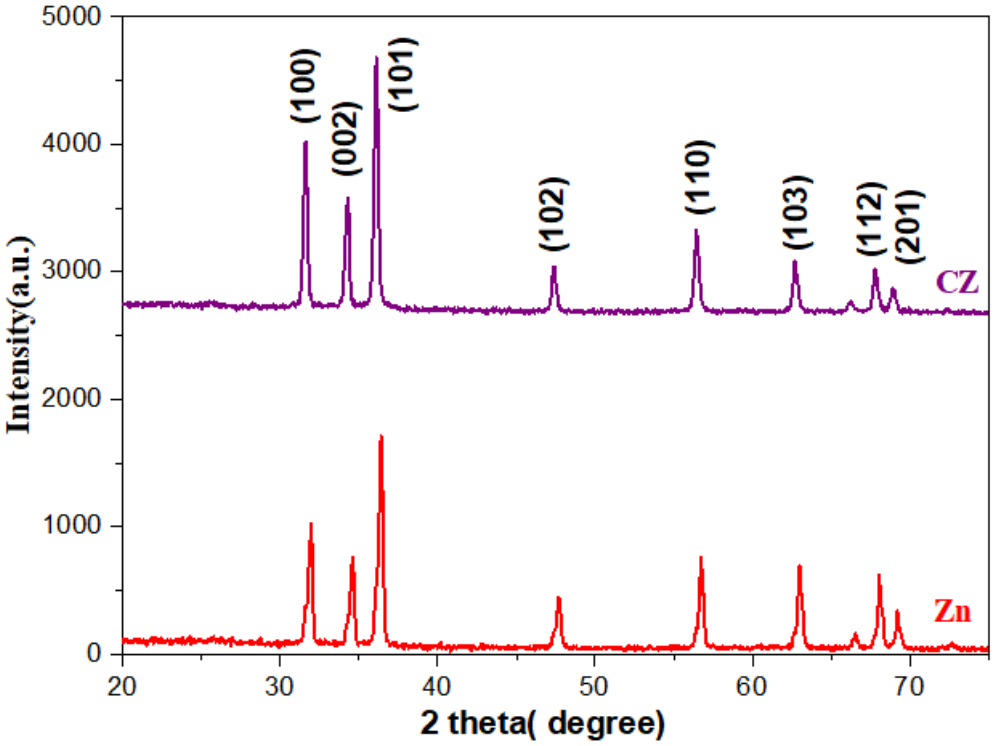

Figure5.1: XRD spectra of ZnO and Cu doped ZnO nanorod synthesized by hydrothermal method

Sample ID	Debye Scherrer method	
	D(nm)	Strain(Є) (10^{-3})
Zn	26.86512	0.340688135
CZ	24.44796	0.356191803

Table 1 : Crystalline size and strain calculated from Debye Scherrer formula

Optical studies

Room temperature Ultraviolet Visible(UV-Vis) absorption spectra of pure ZnO and Cu doped ZnO samples are shown in figure. For all the samples, the spectra shows peaks in UV region. Using Tauc relation, band gap energy can be calculated[10] .

$$\alpha h\vartheta = A\left(h\vartheta - E_g\right)^n$$

Where A is the proportionality constant, h is planck's constant, ϑ is the frequency of incident photon in Hz, E_g is the bandgap energy in eV and n is the power factor which has values ½ for direct allowed transitions, 3/2 for direct forbidden and 2 or 3 for indirect allowed or indirect forbidden transitions.

By plotting incident photon energy (hϑ) versus $(\alpha h\vartheta)^2$ and extrapolating the curve, the band gap energies of the samples can be calculated. The energy was calculated as 3.18 and 3.22 eV for Zn and CZ respectively. The variation in band gap energy with Cu doping may arises as a result of increase in strain which is due to the increase in number of unit cell per particle.

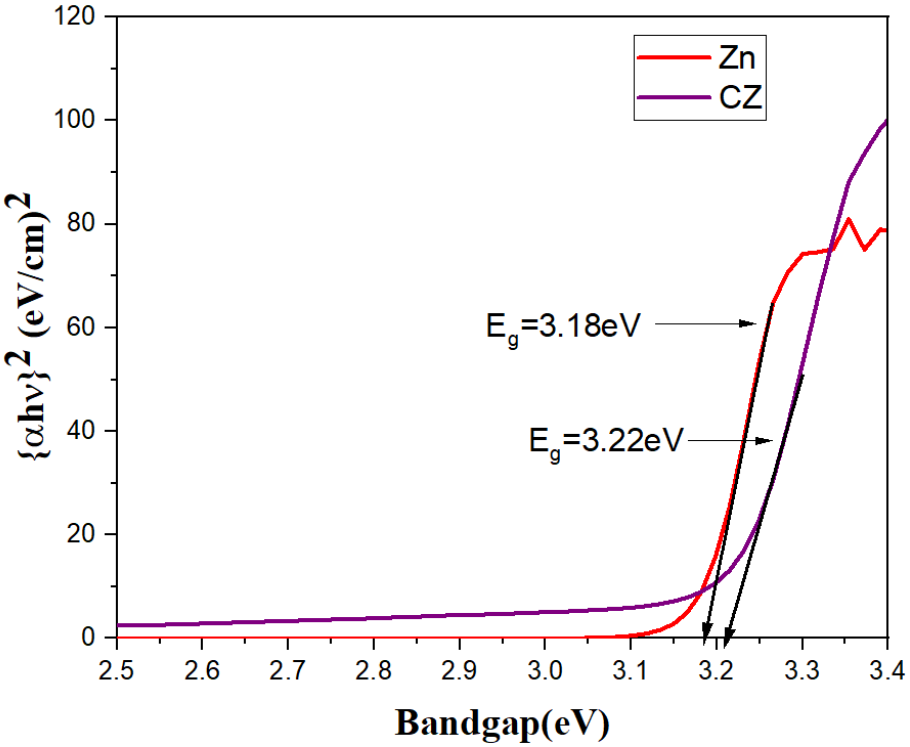

Figure 5.2: Tauc plot corresponding to ZnO and Co doped ZnO nanorod synthesized by hydrothermal method

SEM Analysis

SEM analysis is taken for the surface morphological studies of the prepared samples which include the shape, size , growth mechanism of the samples . SEM micrographs of the prepared samples are shown in figure (3) Zn and CZ. All the three samples shows a rod shaped morphology[11].

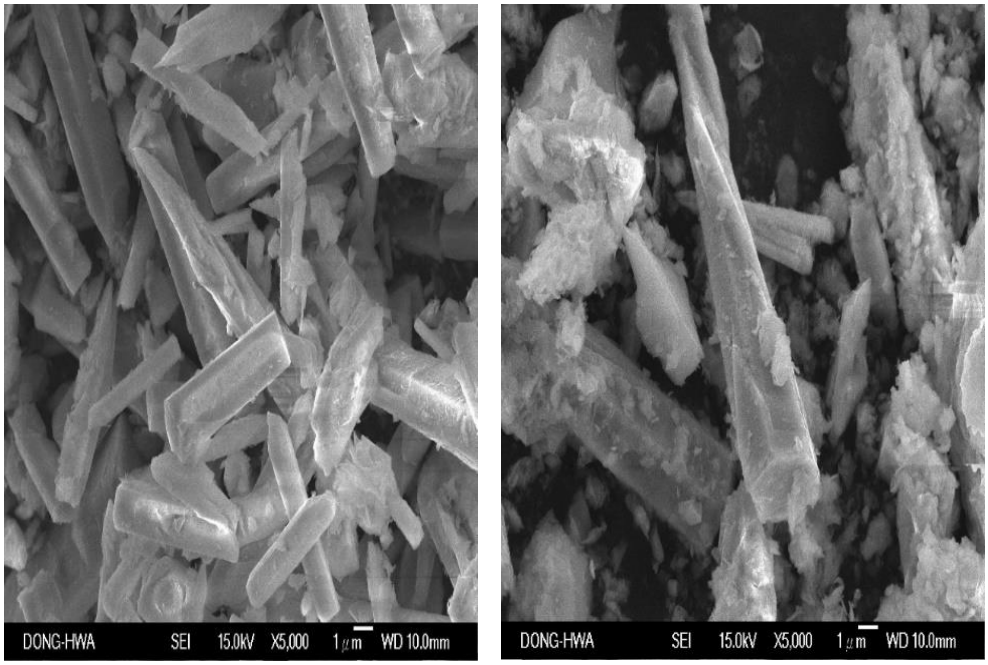

Figure 5.3: SEM images of ZnO(left) and Cu doped ZnO (right) nanorod.

Antibacterial Study

Semiconductor metal oxides are widely used for the antibacterial studies. Here Agar well diffusion method is used to carry out the antibacterial performance of Cu doped ZnO nanoparticle against various bacterial strain. The zone of inhibition of pure and Cu doped ZnO samples against Staphylococcus aureus, Pseudomonas aeruginosa, Bacillus cereus is tabulated below.

The results shows that Cu doped ZnO nanoparticle exhibits an inhibition to growth of bacterial over a region of 7 to 9mm. CZ shows better antibacterial potential compared to pure. Inhibition zone found an enhancement over high Cu concentration. It is also noted that the antibacterial potential of nanoparticle over Gram positive bacteria is more when compared to gram negative bacteria's which is well matched with the earlier reports [12]. The combined effect of $Cu^{2+,}$ Zn^{2+} ions with negative sites of bacteria results in the cell death.

Sample ID	Staphylococcus aureus	Pseudomonas aeruginosa	Bacillus cereus
Zn	8mm	7mm	9mm
CZ	8mm	8mm	9mm

Table 2: Antibacterial study of Zn and CZ on various bacterial strains.

Chapter 6

CONCLUSION

ZnO and Cu doped ZnO nanoparticles were successfully synthesized by hydrothermal method. This sample was characterized using characterization techniques such as

1.X- Ray Diffraction (XRD)

2. Field Emission Scanning Electron Microscopy(FESEM)

3.UV spectroscopy

Antibacterial potential of the samples were also investigated over various bacterial strains.

• From XRD analysis, peaks corresponmding to pure and Cu doped ZnO seems to be matching very well with the standard data.The sharp diffraction peaks indicate the highly crystalline nature of the material. For doped samples the increase in strain compared to the pristine ZnO causes the increase in lattice constants and thereby there is a decrease in particle size observed.

• FESEM analysis shows the surface morphological studies of the prepared samples which shows a rod shaped morphology

• UV spectroscopic study shows the room temperature UV Visible absorption spectra of pure ZnO and Cu doped ZnO samples .For all the samples in spectra shows peaks in UV region . band gap energy found to increase with doping.

•Antibacterial study reveals that Cu doped ZnO nanoparticle exhibits an inhibition to growth of selected bacterias over a region of 7 to 9 mm. CZ shows better antibacterial potential compared to pure sample.

REFERENCES

[1].S.Muthukumaran,R Gopalakrishnan " structural,FTIR and Photoluminescence studies of Cu doped ZnO nanopowders" by co-precipitation method,optical materials 34(2012) 1946-1953.

[2].Susmi Anna Thomas ,Sujit Anil Kadam , Lolly Maria Jose ,Yuan-Ron Ma,D.Sajan and Arun Aravind ," Investigation of adsorption and photocatalytic behaviour of Manganese doped ZnO nanostructures".

[3].Lolly Maria Jose, R S Arun Raj, D Sajan ,Arun Aravind , " Adsorption and photocatalytic activity of biosynthesised ZnO nanoparticles using aloe-vera leaf extract".Nanoexpress to (2021)010039.

[4].Sonima Mohan ,Mini Vellakat,Arun Aravind ,Reka U,"Hydrothermal synthesis and characterization of ZnO nanoparticles of various shapes under different reaction conditions",Nanoexpress1(2020)030028

[5].Afshin Maleki, Mahdi Safari , Behzad Shamoradi,Yahya Zandsalimi,Hiua Daraei, Fardin Gharibi,"Photocatalytic degradation of humic substances is aqueous solution using Cu doped ZnO nanoparticles under natural sunlight irradiation",DOI 10.1007/s11356-015-4915-7

[6].L Ben Saad , L.Soltane, F.Sediri " Pure and Cu doped ZnO nanoparticles : Hydrothermal synthesis, structural and optical properties",Doy:10.1134/S0036024419130259

[7] P. Raju, D. Deivatamil, John Abel Martin Mark, Joseph Prince Jesuraj, Antibacterial and catalytic activity of Cu doped ZnO nanoparticles: structural, optical, and morphological study, Journal of the Iranian Chemical Society, (2021), https://doi.org/10.1007/s13738-021-02352-3

[8]Sonal Singhal , Japinder Kaur, Tsering Namgyal, Rimi Sharma, Cu-doped ZnO nanoparticles: Synthesis, structural and electrical properties, Physica B 407 (2012) 1223-1226

[9]Min Fua, Yalin Li ,Siwei wu, Peng Lu, Jing Liu, Fan Dong, Sol–gel preparation and enhanced photocatalytic performance of Cu-doped ZnO nanoparticles, Applied Surface Science 258 (2011) 1587–1591.

[10]Vipul J. Shukla & Amit Patel (2020) Synthesis, optical, and photoluminescence properties of undoped and Cu-doped ZnO thin films by colloidal solution route, Molecular Crystals and Liquid Crystals, 712:1, 62-75, DOI: 10.1080/15421406.2020.1856505.

[11]Wen Dai, Xinhua Pan, Cong Chen, Shanshan Chen, Wei Chen, Honghai Zhang and Zhizhen Ye, Enhanced UV detection performance using a Cu doped ZnO nanorod array film†, RSC Adv., 2014, 4, 31969, DOI: 10.1039/c4ra04249b.

[12Khalid A, Ahmad P, Alharthi AI, Muhammad S, Khandaker MU, Faruque MRI, et al. (2021) Synergistic effects of Cu-doped ZnO nanoantibiotic against Gram-positive bacterial strains. PLoS ONE 16(5): e0251082. https://doi. org/10.1371/journal.pone.0251082.